

# *Studies of the discharge mechanisms in electrochemical arc machining*

I. M. CRICHTON, J. A. McGEOUGH

*Department of Mechanical Engineering, University of Edinburgh, Edinburgh, UK*

Received 21 July 1983; revised 8 May 1984

The electrochemical arc machining (ECAM) process combines features of ECM and EDM by application of a pulsed voltage between a cathode-tool and anode-workpiece in a liquid electrolyte. The new process offers rates of metal removal as much as five and fifty times greater than ECM and EDM, respectively. The study reported in this paper explores some of the fundamental processes which occur during ECAM. Experimental apparatus was constructed to enable single pulse discharges to be studied. Results are presented for 200  $\mu$ s pulses between 2 mm diameter silver steel electrodes in NaNO<sub>3</sub> and NaCl electrolytes over a gap range of 10 to 90  $\mu$ m. Four stages of electrical phenomena were distinguished within a pulse: (a) high frequency voltage and current oscillations, (b) high rate electrochemical action, (c) low rate electrochemical action, and (d) electrodischarge action. The relative durations of the electrochemical and discharge phases, respectively, increase and decrease with increasing gap width, and vary with electrolyte type and concentration. High speed photography with an image-converter camera was used to record the occurrence of both spark and arc discharge in an electrolyte.

## 1. Introduction

This study is a contribution to fundamental studies of an electrochemical arc machining (ECAM) process which combines features of electrochemical (ECM) and electrodischarge (EDM) machining. The new ECAM process relies on electrical discharges of relatively long time duration in an electrolyte to erode metal from an anodically-polarized workpiece at rates which can be as much as five and fifty times greater than, respectively, ECM and EDM.

Much has been published on the discharges that occur in liquid dielectrics and their relevance to EDM. Crichton *et al.* [1] have reviewed the literature in this field and, with so little published in the field of discharges in electrolytes, have discussed its relevance to the ECAM process.

Applications in which a combined form of EDM and ECM has been used in hole-drilling have been described by Kubota and Tamura [2], Kubota [3] and by Drake and McGeough [4]. Kubota and co-workers have also studied the effects of single pulses of duration 4–80 ms in electrolytes [5, 6]. They conclude that when a

voltage pulse is applied across electrodes in an electrolyte three conditions may occur: an electrochemical reaction only; or electrochemical reactions accompanied by either spark or arc discharges. The former type of discharge occurs between the cathode electrode and the electrolyte solution through bubbles formed by the electrochemical reaction; this may occur irrespective of the gap width. On the other hand an arc discharge is formed when a spark grows to bridge the two electrodes. They report that a spark discharge has no effect on metal removal, and that an arc discharge leaves a crater on the workpiece surface. They also found that the ignition delay decreases with rise in electrolyte concentration, attributing this effect to increased electrolytic current and consequently to a greater rate of gas bubble formation.

The effects of much shorter pulses, of duration 200  $\mu$ s, form the basis of this investigation, with the main interest centred on the phenomena which occur prior to discharge. This pulse length, typical of that used for EDM 'roughing', was the maximum available streak time of the image-converter camera. Also, studies of the conditions

leading up to the onset of discharges in ECAM should throw valuable light on the most appropriate conditions for initiating the process.

Confusion often arises over the difference between arcs and sparks. In EDM, arcing refers to the undesirable condition where successive discharges no longer occur at random throughout the working gap, but stabilize at one position, causing damage to both electrode and workpiece. The cause of this is likely to be inadequate flushing of the process debris. On a single pulse basis, however, a more formal definition is required. Rudorff [7] describes a spark as a sudden transient and noisy discharge between two electrodes; an arc being a stable thermionic phenomenon. This definition is in agreement with the findings of Battacharyya and El-Menshawy [8, 9], who showed that radio frequency energy during sparking is much greater than during arcing. In addition, a series of sparks can take place, and the position of the sparks may alter during a single pulse.

## 2. Apparatus and procedure

### 2.1. Discharge cell

Fig. 1 shows the discharge apparatus.

A Schneeberger Model NK 2-95 frictionless table and the first of two vee-blocks were mounted on a 10 mm thick ground steel base plate. The second vee-block was mounted on the frictionless table, and the vee-blocks were ground to ensure accurate alignment. Tufnol sheet and bushes at the base of each block provided electrical isolation. The ball-end spindle of a Moore and Wright micrometer head operating against the lower end of the frictionless table was used to vary the distance between the vee-blocks. Movement free from backlash was ensured by the weight of the table acting against the spindle.

A small cylindrical test cell of capacity 0.8 ml, with a glass window was mounted on one electrode. The lower section of the threaded two part cell tightened onto an O-ring seal, thus holding the cell in place. Two silver steel rods 2 mm in diameter and 55 mm in length were used as the electrodes. These were inserted into the vee-grooves, with the cell held on the lower electrode. Power leads with brass clamps were then attached,

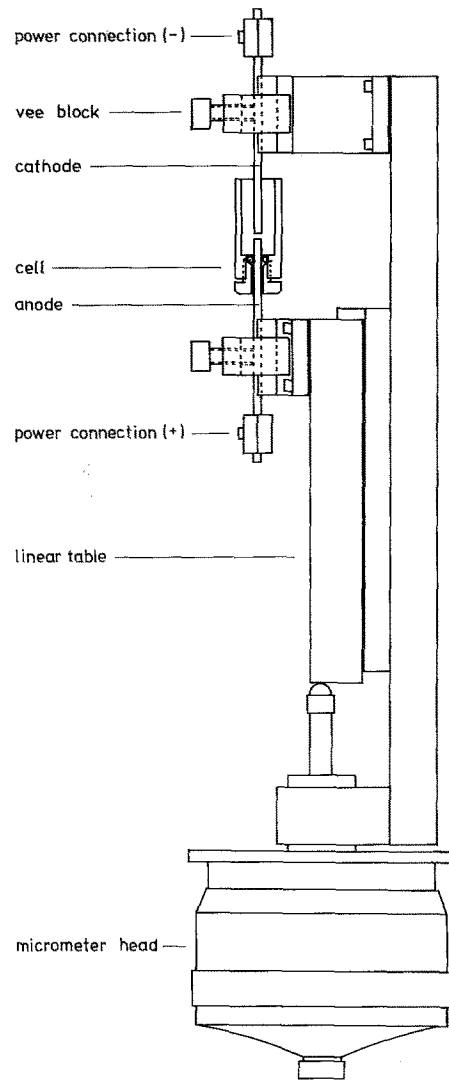


Fig. 1. Discharge apparatus.

and the cell filled with electrolyte (3M NaNO<sub>3</sub> or 3M NaCl solution).

### 2.2. Power supply

A GKN model E pulse generator formed the basis of the power supply. An astable multivibrator of variable pulse duration and duty factor switched an 85 V d.c. power supply through a series of transistor stages, to yield a train of rectangular pulses, with a current output of up to 90 A. This generator was modified to produce a push-button triggered single pulse by replacing the astable circuit with a monostable circuit based on the

555 timer i.c. By control of the monostable R-C time constant output durations from as little as  $25 \mu\text{s}$  could be obtained at various currents, depending on the number of power transistor stages in use. A problem of 'switch bounce' in which the trigger pulse had to be of shorter duration than the output pulse had to be overcome. To that end the monostable was constructed from a 556 i.c. which contains two independent 555 timers with common voltage supply rails. By connecting the output of the first monostable to the input of the second through a  $1 \text{ nF}$  capacitor, sequential timing was obtained. The output pulse set by the time-constant of the second monostable began after  $1.5 \text{ s}$  delay set on the first monostable.

Safe operation was ensured by interfacing the 0–5 V pulse circuit through an opto-isolator to the base of the driver transistor in the GKN generator. (This transistor was connected to a 90 V rail.) The opto-isolator circuit was based on the TIL III i.c. which contains a light emitting diode and a phototransistor, the latter acting as a switch controlled by radiation from the LED. When triggered, the monostable output which is normally 5 V falls to 0 V for the duration of the pulse. The phototransistor then reverts to a non-conducting state, which in turn allows the output stages of the GKN generator to conduct for the duration of the pulse. A cascode circuit by Texas Instruments [10] was included to improve the switching performance of the opto-isolator.

### 2.3. Instrumentation

To measure accurately the pulse current a coaxial shunt based on a design by Grundy [11] and modified by Evans [12] was constructed.

Cross-section detail of the device is shown in Fig. 2. Current flows along the outer tube and returns along the inner resistance tube, both being of non-magnetic material. The potential leads are connected axially on the inner surface of the resistance tube since (by Ampere's circuital law) no magnetic field exists in that region. Copper of outer diameter 15 mm was used for the outer tube with an inner tube made of a resistive alloy of negligible temperature coefficient, and had inner and outer wall diameters of, respectively, 6.2 and 6.4 mm.

A 'resistive' shunt has a series-connected resist-

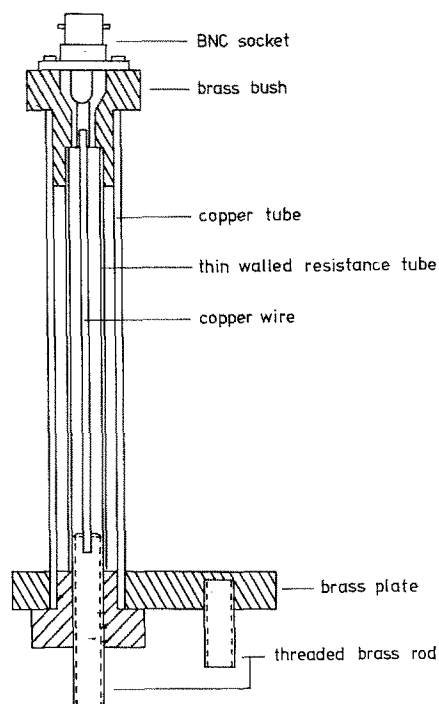


Fig. 2. Coaxial shunt.

ance and inductance as an equivalent circuit. From elementary theory the voltage across it is given by  $v = iR + L(di/dt)$ , in the standard notation. From a d.c. test  $R$  was found to be  $18.2 \text{ m}\Omega$ . The inductance  $L$  measured on a Wayne-Kerr universal bridge, model B234 was found to be less than  $1 \text{ nH}$ . For a current pulse of 90 A with a rise-time of  $2 \mu\text{s}$ , the extreme case in this work, the inductive component is negligible.

### 2.4. Experimental procedure

Prior to each experiment the ends of the electrodes were ground on successively finer grades of wet silicon carbide paper in a Metaserv hand grinder. For this purpose the electrode was inserted into a 25 mm thick steel block which had been drilled through fractionally larger than 2 mm diameter. As the electrode and block were moved over the abrasive surface, light finger pressure was exerted on the protruding end of the electrode. The opposite end was thus ground perpendicular to the centre line, ensuring a parallel gap.

With the electrodes and filled cell in place, and power leads attached, the lower electrode was advanced until it made contact with the fixed

upper electrode. From this condition of zero gap a desired gap was then set by retracting the micrometer spindle, calibrated in  $2\ \mu\text{m}$  divisions. A single pulse was then applied between the electrodes. They were then removed and rinsed prior to examination under an Olympus PMS metallurgical microscope. Voltage and current waveforms during a pulse were recorded on a Gould OS4000 digital storage oscilloscope, with 4001 output unit. The latter device allowed stored waveforms to be plotted on a Gould HR2000  $X$ - $Y$  recorder.

### 3. Experimental results

It was found that on application of an 85 V,  $200\ \mu\text{s}$  pulse, discharge between electrodes immersed in 3 M NaCl or  $\text{NaNO}_3$  electrolyte could be reliably obtained at gaps up to  $90\ \mu\text{m}$ . Similar experiments with paraffin, a common EDM dielectric, revealed that a discharge could not be obtained above  $5\ \mu\text{m}$ . Although these gap ranges would increase considerably under multiple pulse conditions (particularly in the case of a dielectric), the results suggest that it is much easier to initiate a discharge in an electrolyte.

As illustrated in Fig. 3 four stages of electrical phenomena can be distinguished within a single phase.

#### (a) Stage 1

When the voltage pulse is applied, the voltage and current oscillate in phase at high frequency for a short period. The average frequency of oscillation is about 172 and 168 kHz for, respectively,  $\text{NaNO}_3$  and NaCl solutions. Generally, the larger the gap width the longer the duration of this stage.

Kubota *et al.* [6] have also observed oscillations during ignition delay. In their work, frequencies were in the range 9–11 kHz for a 4 ms pulse. They attributed the oscillations to the formation of gas bubbles in the liquid. Using an equation derived by Yokendo [13] they deduced that the bubble radius was about  $20$ – $25\ \mu\text{m}$  maximum, the size of which corresponded to about 40–50% of the gap width. They then assumed that a discharge developed between an electrode and the electrolyte across such a bubble, and that the discharge grew to bridge the electrodes.

When Yokendo's equation is used in the present work a bubble radius of approximately  $1\ \mu\text{m}$  is

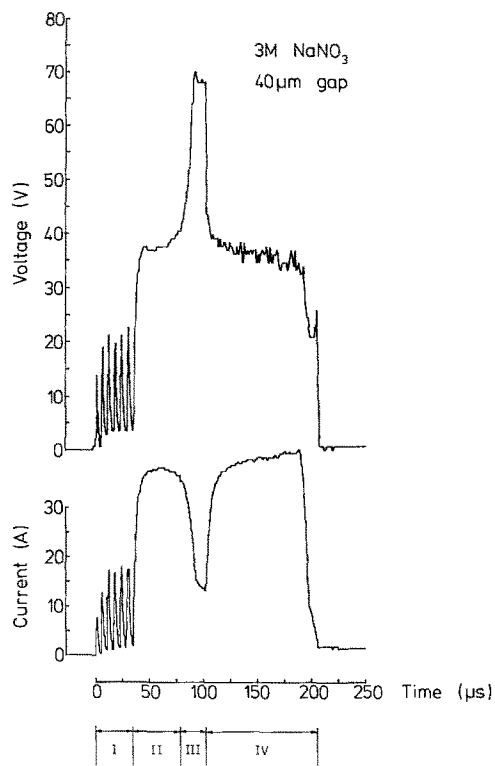


Fig. 3. Electrical phenomena during ECAM with a square-wave pulse.

calculated, for oscillation frequencies of 168–172 kHz. Since the gap width here is of the order of  $10$ – $90\ \mu\text{m}$ , the oscillations in waveform during Stage 1 are not considered to be due to bubbles of this magnitude. Instead, the oscillations may be a consequence of the pulse generator which was used. This was designed as an EDM power supply working with a dielectric fluid. In contrast to EDM, a pulse in ECAM is applied initially across a gap resistance of the order of  $1\ \Omega$ , which will be close to arcing conditions, although a discharge is not yet formed. To prevent electrode damage during unstable conditions, the generator is fitted with circuitry which continually monitors the gap voltage and cuts off the output transistors when arc- or short-circuit conditions occur. The oscillations in Stage 1 may be due to the above circuitry rapidly switching on and off.

#### (b) Stage 2

The oscillations of Stage 1 give rise to a rapid increase in voltage and current to, respectively,

about 30 V and 50 A. ECM is considered to occur during this period causing an accumulation of electrolytic gas or steam within the gap. The volume of gas is such that the current then decreases and the voltage increases, since the mixture of gas with electrolyte in the gap means that the solution acquires the qualities of a dielectric rather than of a conductor. Stage 2 ends with a sudden increase in voltage, tending towards the open-circuit value, accompanied by an abrupt decrease in current.

#### (c) Stage 3

The large proportion of gas in the gap causes the voltage to rise further to about 70 V. A current of 15–25 A still flows due probably to stray ECM which further increases the amount of gas in the gap. At the end of this stage, the voltage drops to about 30 V, whilst the current increases to about 50–60 A, indicating the onset of an electrical discharge. This effect is believed to be associated with gaseous breakdown within a gas bubble.

#### (d) Stage 4

The sudden decrease in voltage and increase in current at the start of Stage 4 mark the onset of a discharge, the duration of which decreases with increasing gap width. The voltage is noted to decrease at the start of the discharge from about 70 to 35 V, and continues to fall slightly throughout the discharge. On the other hand, the current increases throughout the discharge from about 15 to 40 A. Both the voltage and current waveforms exhibit very high frequency oscillations (thought to be much higher than the 225 kHz bandwidth of the storage oscilloscope used), the effect being more marked in the former: these are considered to be due to radio-frequency emission. From this observation, the discharge is believed to be a spark, rather than an arc.

### 3.1. Streak photography of single discharges

Further work was carried out to establish whether these discharges in an electrolyte can be regarded as arcs or sparks. Battacharyya and El-Menshawey [8, 9] have shown that it is possible to distinguish between sparks and arcs during EDM from measurements of the light emission and of the radio frequency (r.f.) emission from the gap. They observed that the r.f. energy during sparking is much greater than that during arcing. Sparks

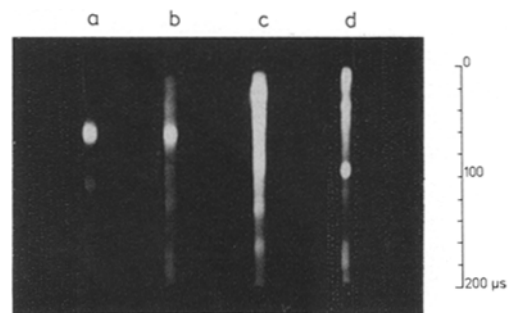


Fig. 4. Streak photographs of discharges in 3M  $\text{NaNO}_3$  electrolyte.

were noted to be noisy and transient, whilst arcs were of constant intensity at a stationary point between the electrodes.

To that end, an STL image converter camera was used to distinguish the type of discharge occurring in the electrolytes used in ECAM. Fig. 4 shows four 200  $\mu\text{s}$  streaks obtained by this method. The discharges were initiated in succession, without changing the electrodes or electrolyte. The uneven light intensity of streaks (a) and (b) indicates a sparking condition. As debris gathers in the gap, streaks (c) and (d) indicate a tendency towards arcing at the beginning of the discharge, by the even light intensity. This work demonstrates that both spark and arc discharges can develop in electrolytes.

### 3.2. Electrochemical and electrodischarge action

Tables 1 and 2 for, respectively,  $\text{NaNO}_3$  and  $\text{NaCl}$  electrolytes show the duration of the four stages within a 200  $\mu\text{s}$  pulse as gap width is varied.

Table 1. Time duration of electrical phenomena within a 200  $\mu\text{s}$  pulse in 3M  $\text{NaNO}_3$  electrolyte

Gap ( $\mu\text{m}$ )	Stage 1 ( $\mu\text{s}$ )	ECM		EDM Stage 4 ( $\mu\text{s}$ )
		Stage 2 ( $\mu\text{s}$ )	Stage 3 ( $\mu\text{s}$ )	
10	22.5	25.0	25.0	147.5
20	35.0	30.0	15.0	122.5
30	35.0	35.0	25.0	107.5
40	37.5	35.0	30.0	105.0
50	47.5	30.0	50.0	77.5
60	57.5	37.5	40.0	82.5
70	52.5	35.0	45.0	70.0
80	47.5	35.0	65.0	60.0
90	47.5	35.0	90.0	27.5

Table 2. Time duration of electrical phenomena within a 200  $\mu\text{s}$  pulse in 3M NaCl electrolyte

Gap ( $\mu\text{m}$ )	Stage 1 ( $\mu\text{s}$ )	ECM		EDM Stage 4 ( $\mu\text{s}$ )
		Stage 2 ( $\mu\text{s}$ )	Stage 3 ( $\mu\text{s}$ )	
10	25.0	20.0	10.0	162.5
20	42.5	7.5	10.0	147.5
30	35.0	12.5	15.0	137.5
40	30.0	17.5	15.0	137.5
50	32.5	17.5	12.5	140.0
60	35.0	20.0	32.5	120.0
70	35.0	25.0	22.5	122.5
80	35.0	25.0	32.5	107.5
90	60.0	17.5	45.0	75.0

Stage 1 accounts for 22–60  $\mu\text{s}$ , during which metal removal is likely to be minimal. This represents 11–30% of a 200  $\mu\text{s}$  pulse, but becomes less significant with increasing pulse length. It may be that the oscillatory phenomenon can be eliminated by circuit modification. (Further work has shown this to be the case.) Stages 2 and 3 represent electrochemical action (at different rates), and Stage 4 electrodischarge action. The durations of these ECM and EDM phases within a 200  $\mu\text{s}$  pulse are shown graphically in Figs. 5 and 6 for, respectively,  $\text{NaNO}_3$  and NaCl electrolytes.

Fig. 5 shows that the discharge action (EDM) predominates over ECM for the smaller gaps, up to about 55  $\mu\text{m}$ , but that above this gap, ECM has the greater effect (on a time basis). In contrast,

Fig. 6 shows that the discharge action always has a greater effect than ECM for NaCl solution. With the latter electrolyte, the conductivity is greater than for  $\text{NaNO}_3$  of the same concentration. Thus a higher current is produced, and more gas is evolved than is obtained with  $\text{NaNO}_3$  solution. The greater the abundance of gas within the inter-electrode gap, the greater is the amount of the discharge action. This result is consistent with that of Kubota *et al.* [6] who observed that the ignition delay decreases as the electrolyte concentration and conductivity is increased.

Both electrolytes exhibit the general trend that within a 200  $\mu\text{s}$  pulse, the proportions of ECM and EDM, respectively, increase and decrease with increasing gap width. The larger the gap, the higher is the voltage required to initiate discharge action across it. Thus ECM action predominates for these conditions. The smaller the inter-electrode gap, the greater the amount of gas bubbles that is produced, and a smaller ignition delay is needed to initiate the spark action across it. EDM type action has therefore the greater effect at these conditions.

#### 4. Conclusions

Electrical discharges in an electrolyte occur across localized regions of evolved gas and/or electrolyte vapour. High speed photography has shown that both spark and arc discharges are possible in an electrolyte. The type of discharge may be distinguished from the energy of emitted radio frequencies or by the study of the light emitted. On

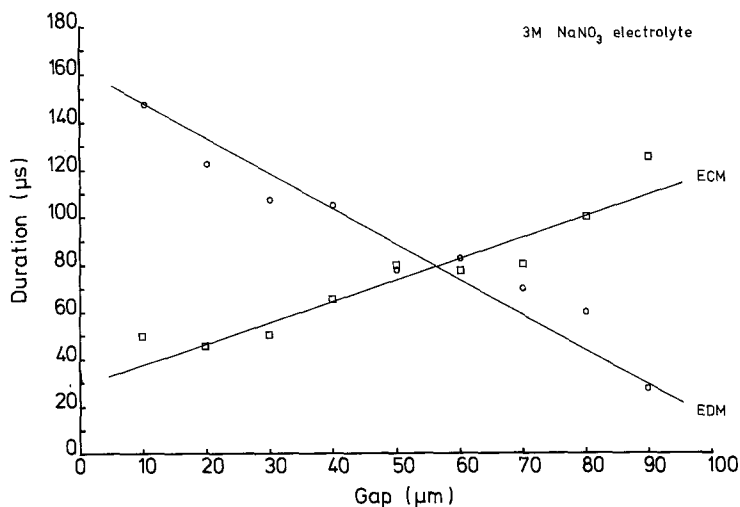


Fig. 5. Variation of ECM and EDM phases with gap, during a 200  $\mu\text{s}$  pulse.

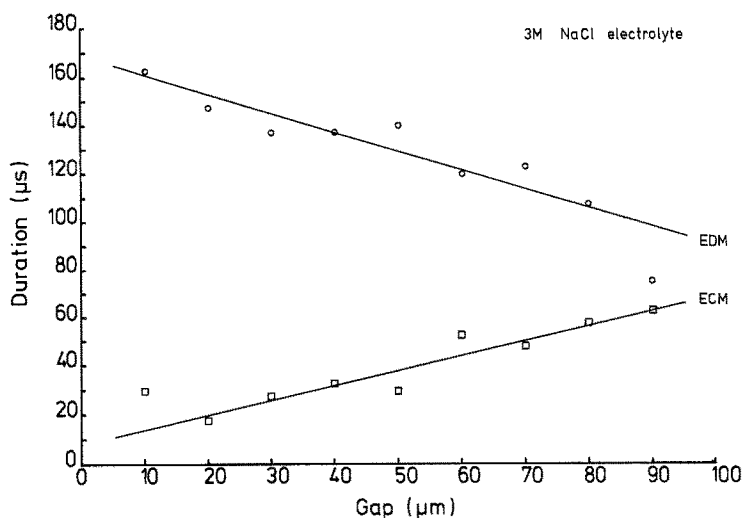


Fig. 6. Variation of ECM and EDM phases with gap, during a 200  $\mu\text{s}$  pulse.

application of a voltage pulse between two electrodes immersed in an electrolyte, three phenomena may occur: (a) electrochemical action only, (b) electrochemical action followed by discharge between an electrode and the electrolyte, and (c) electrochemical action followed by discharge between the electrodes.

Within the single pulse voltage and current waveforms obtained with phenomenon (c), four electrical stages may be distinguished: (1) high frequency oscillations (170 kHz), (2) high rate ECM, (3) low rate ECM and (4) electrical discharge. Stage 1 represents an unproductive period; however further work has shown that it may be eliminated by circuit modification. Stages 2 and 3 together represent an ECM phase, and Stage 4 an EDM phase. The durations of these phases respectively increase and decrease with increasing gap width, and vary with electrolyte type, concentration and conductivity. Under suitable gap conditions a discharge between an electrode and an electrolyte solution may easily develop to bridge the electrodes. This observation may provide the explanation why discharges in an electrolyte occur over a wider range of gaps than for a dielectric.

## References

- [1] I. M. Crichton, J. A. McGeough, W. Munro and C. White, *Precision Eng.* 3 (1981) 155.
- [2] M. Kubota and Y. Tamura, *Bull. Jpn Soc. Precis. Eng.* 7 (1973) 114.
- [3] M. Kubota, *Mechanique* 303 (1975) 15.
- [4] T. Drake and J. A. McGeough, 'Proceedings of the Machine Tool Design Conference', MacMillan Publishers Ltd, London (1981) pp. 363-9.
- [5] M. Kubota, Y. Tamura, J. Omori and Y. Hirano, *J. Assoc. Electro-Mach.* 12 (1978) 24.
- [6] M. Kubota, Y. Tamura, H. Takahashi and T. Sugaya, *ibid.* 13 (1980) 42.
- [7] D. W. Rudorff, *Proc. I. Mech. Eng.* 171 (1957) 495.
- [8] S. K. Battacharyya and M. F. El-Menshawy, Identification of the discharge profile in EDM in 'Sixth North American Metal-working Research Conference', University of Florida, 16, 17 April, 1978.
- [9] *Idem*, *Int. J. Prod. Res.* 16 (1978) 353.
- [10] Texas Instruments, 'The Optoelectronics Data Book for Design Engineers', (Texas Instruments, London, 1972).
- [11] J. A. Grundy, *Proc. IEE* 124 (1977) 499.
- [12] P. D. Evans, personal correspondence (1980).
- [13] Yokendo, Kansai Branch of the Association of Electromachinery, Japan (1976) p. 22.